AIRCRAFT ENGINE RUN-TO-FAILURE DATASET UNDER REAL FLIGHT CONDITIONS

Manuel Arias Chao
ETH Zurich
manuel.arias@ethz.ch

Chetan Kulkarni
KBR, Inc., NASA Ames Research Center
chetan.s.kulkarni@nasa.gov

Kai Goebel
Luleå University of Technology
kai.goebel@ltu.se

Olga Fink
ETH Zurich
ofink@ethz.ch

April 20, 2020

The generation of data-driven prognostics models requires the availability of datasets with run-to-failure trajectories. In order to contribute to the development of these methods, the dataset provides a new realistic dataset of run-to-failure trajectories for a small fleet of aircraft engines under realistic flight conditions. The damage propagation modelling used for the generation of this synthetic dataset builds on the modelling strategy from previous work [1] and incorporates two new levels of fidelity. First, it considers real flight conditions as recorded on board of a commercial jet [2]. Secondly, it extends the degradation modelling by relating the degradation process to the operation history. The dataset was generated with the Commercial Modular Aero-Propulsion System Simulation (C-MAPSS) dynamical model [3]. More details about the generation process can be found in [4].

1 Introduction

An important requirement for the generation of realistic run-to-failure trajectories is the availability of a suitable system model that allows variations of sub-system component health and the simulation of the output sensor measurements. The C-MAPSS (Commercial Modular Aero- Propulsion System Simulation) dynamical model [3] has been used in the past for degradation modelling in [1]. However, the run-to-failure trajectories provided in this previous work are restricted to six possible operative snapshots during cruise. In addition, the onset of an abnormal degradation is not dependent on the past operative profile. Therefore, the resulting degradation trajectories lack important factors of complexity that are present in real systems. In [4] we used the same CMAPSS dynamical model and extended the degradation modelling to address these limitations. This document presents usage of the dataset using one of the resulting datasets from the simulation data and used in [5].

2 CMAPSS Model

The CMAPSS dynamical model is a high fidelity computer model for simulation of a realistic large commercial turbofan engine. Figure 1 shows an schematic representation of the engine along with the corresponding station numbers that is used in the CMAPSS documentation [3]. In addition to the engine thermodynamic model, the package includes an atmospheric model capable of operation at (i) altitudes from sea level to 40,000 ft, (ii) Mach numbers from 0 to 0.90, and (iii) sea-level temperatures from –60 to 103 °F. The package also includes a power-management system that allows the engine to be operated over a wide range of thrust levels throughout the full range of flight conditions. The resulting operation envelope is shown in Figure 2.

We refer to the mathematical abstraction of the CMAPSS computer models as the system model which has the form of a coupled system of nonlinear equations. The inputs of the system model are divided into scenario-descriptor operating conditions w and unobservable model health parameters θ. The outputs of the system model are estimates of the measured physical properties $\hat{x}_s$ and unobserved properties $\hat{x}_v$ that are not part of the condition monitoring signals (i.e.,

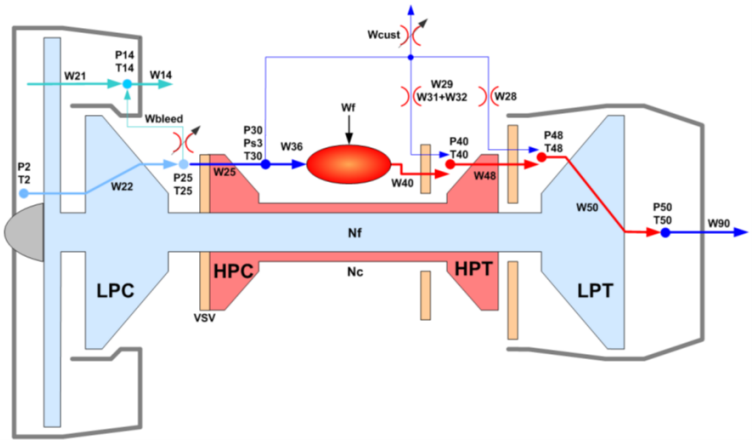

Figure 1: Schematic representation of CMAPSS model [3]

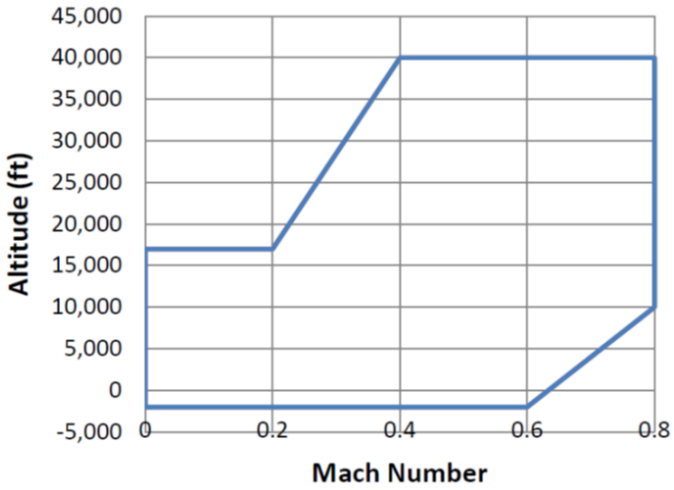

Figure 2: Flight envelope [3]

virtual sensors). The nonlinear system model is denoted as:

$$[\hat{x}_s^{(t)}, \hat{x}_v^{(t)}] = S(w^{(t)}, \theta^{(t)}) \tag{1}$$

The unobservable model health parameters θ are model tuners and they fall in the class called quality parameters (i.e., component efficiencies, flow, input Scalars, output Scalars, and/or adders).

Tables 2 to 4 provide the name, description and units of each input variable in the dataset. The variable symbol corresponds to the internal variable name in CMAPSS. The descriptions and units are reported as in the model documentation [3].

Table 1: Scenario descriptors (i.e Flight Data) - $[w]$

#	Symbol	Description	Units
1	alt	Altitude	ft
2	Mach	Flight Mach number	-
3	TRA	Throttle-resolver angle	%
4	T2	Total temperature at fan inlet	°R

Table 2: Measurements - $[x_s]$

Id	Symbol	Description	Units
5	Wf	Fuel flow	pps
6	Nf	Physical fan speed	rpm
7	Nc	Physical core speed	rpm
8	T24	Total temperature at LPC outlet	°R
9	T30	Total temperature at HPC outlet	°R
10	T48	Total temperature at HPT outlet	°R
11	T50	Total temperature at LPT outlet	°R
12	P15	Total pressure in bypass-duct	psia
13	P21	Total pressure at fan outlet	psia
14	P24	Total pressure at LPC outlet	psia
15	Ps30	Static pressure at HPC outlet	psia
16	P40	Total pressure at burner outlet	psia
17	P50	Total pressure at LPT outlet	psia

Table 3: Virtual Sensors - $[x_v]$

#	Symbol	Description	Units
18	T40	Total temp. at burner outlet	°R
19	P30	Total pressure at HPC outlet	psia
20	P45	Total pressure at HPT outlet	psia
21	W21	Fan flow	pps
22	W22	Flow out of LPC	lbm/s
23	W25	Flow into HPC	lbm/s
24	W31	HPT coolant bleed	lbm/s
25	W32	HPT coolant bleed	lbm/s
26	W48	Flow out of HPT	lbm/s
27	W50	Flow out of LPT	lbm/s
28	epr	Engine pressure ratio (P50/P2)	–
29	SmFan	Fan stall margin	–
30	SmLPC	LPC stall margin	–
31	SmHPC	HPC stall margin	–
32	NRf	Corrected fan speed	rpm
33	NRc	Corrected core speed	rpm
34	PCNfR	Percent corrected fan speed	pct
35	phi	Ratio of fuel flow to Ps30	pps/psi

3 Dataset Overview - A Small Fleet of Turbofan Engines

The dataset documented in this work provides synthetic run-to-failure degradation trajectories of a small fleet comprising nine turbofan engines with unknown and different initial health conditions. Real flight conditions as recorded on board of a commercial jet were taken as input to the C-MAPSS model [2]. Figure 3 shows the kernel density estimations of the simulated flight envelopes given by the scenario-descriptor variables W: altitude (alt), flight Mach number (XM), throttle-resolver angle (TRA) and total temperature at the fan inlet (T2) for $N = 6$ training units ($u = 2$, 5, 10, 16, 18 & 20) and $M = 3$ test units ($u = 11$, 14 & 15). It is worth noticing that test units 14 and 15 have an operation distribution that is significantly different from training units. Concretely, test units 14 and 15 operate shorter and lower altitude flights compared to other units. The training dataset, therefore, contains flight profiles that are not fully representative for the test conditions of these two units.

An example of a typical single flight cycle given by traces of the scenario-descriptor variables is shown in Figure 4. Each flight cycle contains recordings of varying lengths, covering climb, cruise and descend flight conditions (with alt > 10000 ft) corresponding to different flight routes operated by the aircraft. The remaining units of the fleet follow similar flight traces.

Two distinctive failure modes are present in the available dataset ($\mathcal{D}$). Units 2, 5 and 10 have failure modes of an *abnormal* high pressure turbine (HPT) efficiency degradation. Units 16, 18 and 20 are subject to a more complex failure mode that affects the low pressure turbine (LPT) efficiency and flow in combination with the high pressure turbine

Table 4: Model Health Parameters - $[\theta]$

#	Symbol	Description	Units
36	fan_eff_mod	Fan efficiency modifier	-
37	fan_flow_mod	Fan flow modifier	-
38	LPC_eff_mod	LPC efficiency modifier	-
39	LPC_flow_mod	LPC flow modifier	-
40	HPC_eff_mod	HPC efficiency modifier	-
41	HPC_flow_mod	HPC flow modifier	-
42	HPT_eff_mod	HPT efficiency modifier	-
43	HPT_flow_mod	HPT flow modifier	-
44	LPT_eff_mod	LPT efficiency modifier	-
45	LPT_flow_mod	HPT flow modifier	-

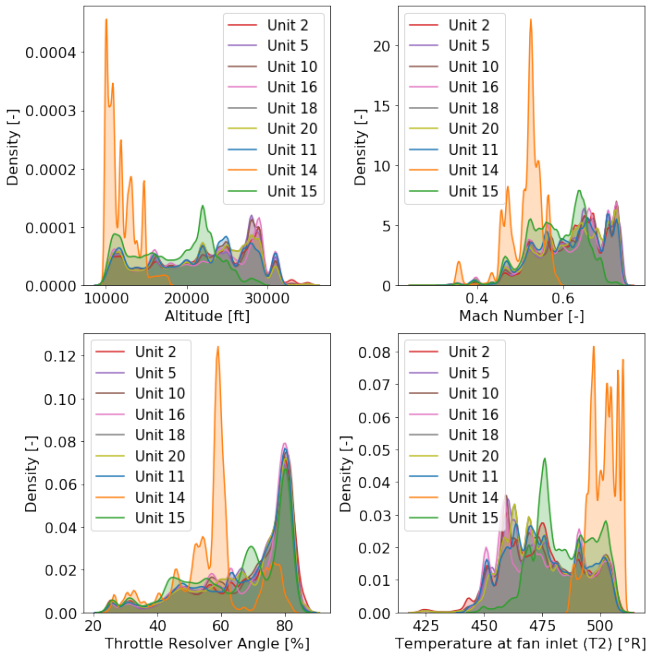

Figure 3: Kernel density estimations of the simulated flight envelopes given by recordings of altitude, flight Mach number, throttle-resolver angle (TRA) and total temperature at the fan inlet (T2). The complete run-to-failure trajectories of nine fleet units are shown. $N = 6$ training units ($u = 2$, 5, 10, 16, 18 & 20) and $M = 3$ test units ($u = 11$, 14 & 15) are represented. Test Unit 11 (blue) has a similar operation profile as the training units. Test units 14 (orange) and Unit 15 (green) operate shorter and lower altitude flights.

(HPT) efficiency degradation. Test units are subjected to the same complex failure mode. Figure 6 shows degradation profiles induced in the nine units of the fleet. The initial deterioration of each unit is different and corresponds to an engine-to-engine variability equivalent to a 10% of the health index. The degradation of the affected system components follows a stochastic process with a linear *normal degradation* followed by a steeper *abnormal degradation*. The degradation rate of each component varies within the fleet. The transition from *normal* to *abnormal* degradation is smooth and occurs at different cycle times for each unit. The transition time (t_s) is dependent on the operating condition i.e., flight and degradation profile. It should be noted that although the degradation profiles of individual components show nearly overlapping trajectories, the combined profile i.e., the profile in the three dimensions is clearly different. More details about the generation process can be found in [4].

An overview of the transition times t_s, the end-of-life times t_{EOL} and the number of samples from each unit of the fleet m_i is provided in Table 5. The sampling rate of the data is 1Hz resulting in a total size of the dataset of 5.3M samples for training and 1.2M samples for testing. It is worth noticing that while test unit 14 is a short flight engine with the lowest amount of flight time (0.16M seconds) it has the largest number of flight cycles.

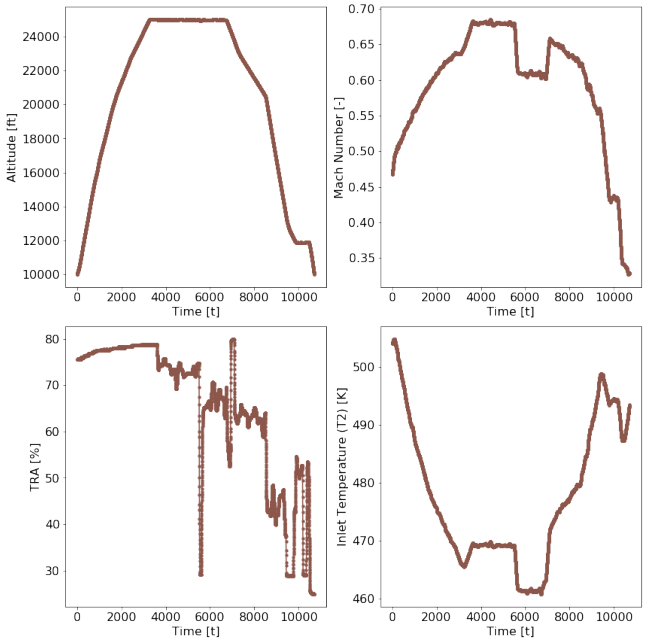

Figure 4: Single flight traces of altitude, flight Mach number (XM), throttle-resolver angle (TRA) and total temperature at the fan inlet (T2) for Unit 10. Climb, cruise and descend flight conditions (alt $>$ 10000 ft) are covered.

Available Dataset - $\mathcal{D}$				
Unit (u)	m_i	t_s	t_{EOL}	Failure Mode
2	0.85M	17	75	HPT
5	1.03M	17	89	HPT
10	0.95M	17	82	HPT
16	0.77M	16	63	HPT+LPT
18	0.89M	17	71	HPT+LPT
20	0.77M	17	66	HPT+LPT
Test Dataset - $\mathcal{D}_{T*}$				
Unit (u)	m_j	t_s	t_{EOL}	Failure Mode
11	0.66M	19	59	HPT+LPT
14	0.16M	36	76	HPT+LPT
15	0.43M	24	67	HPT+LPT

Table 5: Size (m_u), the transition cycle time (t_s) and end-of-life time (t_{EOL}) of each unit within the available ($\mathcal{D}$) and test datasets ($\mathcal{D}_{T*}$).

4 Application Scenario

4.1 Prognostics Problem

The formulation of the prognostics problem proposed for this dataset is formally introduced in the following. Given are multivariate time-series of condition monitoring sensors readings $X_{s_i} = [x_{s_i}^{(1)}, \ldots, x_{s_i}^{(m_i)}]^T$ and their corresponding RUL i.e., $Y_i = [y_i^1, \ldots, y_i^{m_i}]^T$ from a fleet of N units ($i = 1, \ldots, N$). Each observation $x_{s_i}^{(t)} \in R^p$ is a vector of p raw measurements taken at operating conditions $w_i^{(t)} \in R^s$. The length of the sensory signal for the *i-th* unit is given by m_i; which can, in general, differ from unit to unit. The total combined length of the available data set is $m = \sum_{i=1}^{N} m_i$. More compactly, we denote the available dataset as $\mathcal{D} = \{W_i, X_{s_i}, Y_i\}_{i=1}^{N}$.

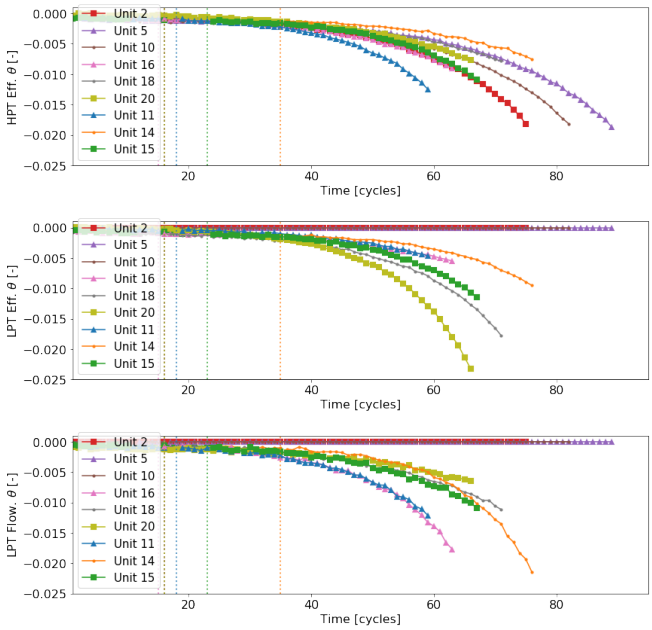

Figure 5: Traces of the degradation imposed on the high pressure turbine efficiency (HPT_Eff_mod), low pressure turbine efficiency (LPT_Eff_mod) and low pressure turbine flow (LPT_flow_mod) for each unit of the fleet. The onset of the abnormal degradation (i.e. t_s) of each unit is indicated by dashed vertical lines.

Given this set-up, the task is to obtain a predictive model $\mathcal{G}$ that provides a reliable RUL estimate ($\hat{\mathbf{Y}}$) on a test dataset of M units $\mathcal{D}_{T*} = \{X_{s_j*}\}_{j=1}^{M}$; where $X_{s_j*} = [x^1_{s_j*}, \ldots, x^{k_j}_{s_j*}]$ are multivariate time-series of sensors readings. The total combined length of the test data set is $m_* = \sum_{j=1}^{M} k_j$.

4.2 Evaluation Metric

Two common evaluation metrics in C-MAPSS prognostics analysis in [1] are proposed to compare the prognostics results: root-mean-square error (RMSE) and NASA's scoring function [1] (s) which are defined as:

$$s = \sum_{j=1}^{m_*} exp(\alpha|\Delta^{(j)}|) \tag{2}$$

$$RMSE = \sqrt{\frac{1}{m_*}\sum_{j=1}^{m_*}(\Delta^{(j)})^2} \tag{3}$$

where m_* denotes the total number of test data samples, $\Delta^{(j)}$ is the difference between the estimated and the real RUL of the j sample (i.e. $y^{(j)} - \hat{y}^{(j)}$) and α is $\frac{1}{13}$ if RUL is under-estimated and $\frac{1}{10}$ otherwise. The resulting s metric is not symmetric and penalizes over-estimation more than under-estimation.

Acknowledgements

This research was funded by the Swiss National Science Foundation (SNSF) Grant no. PP00P2 176878.

References

[1] Abhinav Saxena, Kai Goebel, Don Simon, and Neil Eklund. Damage propagation modeling for aircraft engine run-to-failure simulation. In *2008 International Conference on Prognostics and Health Management*, pages 1–9. IEEE, oct 2008.

[2] DASHlink - Flight Data For Tail 687, 2012.

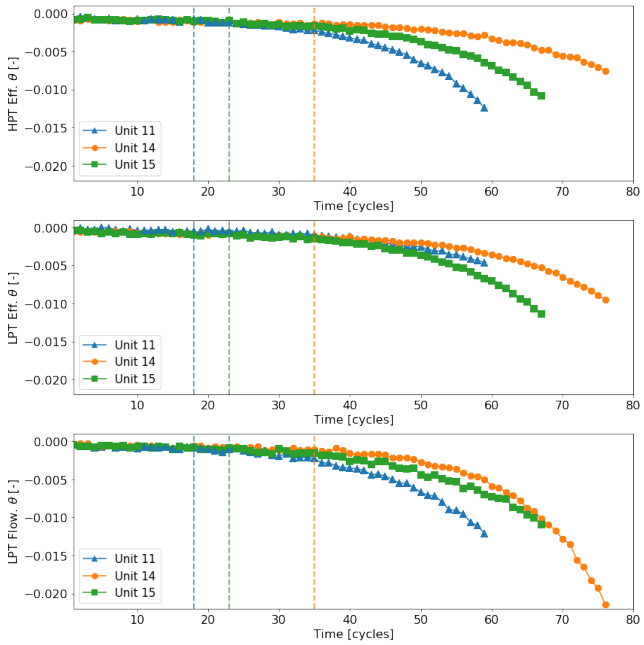

Figure 6: Traces of the degradation imposed to the high pressure turbine efficiency (HPT_Eff_mod), low pressure turbine efficiency (LPT_Eff_mod) and low pressure turbine flow (LPT_flow_mod). Three units are shown: Unit 11 (blue triangle), Unit 14 (green square) and Unit 15 (orange circle). The onset of the *abnormal degradation* (i.e. t_{s_u}) is indicated with dashed vertical lines.

[3] Dean K Frederick, Jonathan A Decastro, and Jonathan S Litt. User's Guide for the Commercial Modular Aero-Propulsion System Simulation (C-MAPSS). Technical report, 2007.

[4] Manuel Arias Chao, Chetan S Kulkarni, Kai Goebel, and Olga Fink. Damage propagation modeling for aircraft engine run-to-failure simulation under real flight conditions. *Under review*, 2020.

[5] Manuel Arias Chao, Chetan Kulkarni, Kai Goebel, and Olga Fink. Fusing physics-based and deep learning models for prognostics, 2020.